



Cite this: *Org. Biomol. Chem.*, 2026, **24**, 2270

Electricity-driven sustainable synthesis of 2-aminobenzonitriles through C–C bond cleavage of isatins: post-functionalization *via* one-pot integration with enzyme catalysis

Kirti Singh,^a Shashi Pandey ^b and Vikas Tyagi ^{*a}

Herein, we report an electricity-mediated sustainable synthesis of 2-aminobenzonitriles, which serve as essential building blocks for numerous pharmaceuticals, by using isatins and hydroxylamine as starting materials. Furthermore, electricity served as an efficient and environmentally friendly mediator, promoting the C–C cleavage of isatin derivatives to afford the desired products in good to excellent yields. The scope and practicality of the method were validated through the screening of isatins bearing different substituents. Moreover, this electrochemical protocol was successfully integrated with an α -amylase-catalyzed aza-Michael addition in a one-pot system, providing pharmaceutically relevant β -aminocarbonyl compounds *via* C–N bond formation. Additionally, mechanistic insights obtained from control experiments and cyclic voltammetry studies suggest that 2-(2-aminophenyl)-2-oxoacetate serves as a key intermediate during the electrochemical step.

Received 24th December 2025,
Accepted 12th February 2026

DOI: 10.1039/d5ob01983d

rsc.li/obc

Introduction

The carbon–carbon bond serves as the fundamental backbone of organic molecules, and its cleavage or functionalization offers an effective way for structural modification.¹ In recent years, considerable attention has been directed toward developing novel and efficient methods for achieving selective C–C bond cleavage. Besides, isatin is recognized as a crucial and privileged scaffold in synthetic chemistry, as it incorporates both a keto group and a lactam moiety within its structure.² The coexistence of these functional groups, along with the easy availability of isatin, makes it a highly versatile starting material for generating clinically important molecules.³ Consequently, a wide range of chemical transformations are being carried out, targeting either the keto or the lactam functionality of isatin to broaden its synthetic and medicinal applications. However, the selective cleavage of C–C bonds in isatin remains relatively underexplored compared to other chemical transformations.⁴ Nevertheless, the molecular scaffolds generated through the selective cleavage of the C–C bond of isatin have significant importance, as they constitute the core structures of various pharmacologically active compounds, including several non-steroidal anti-inflammatory drugs (NSAIDs).⁵

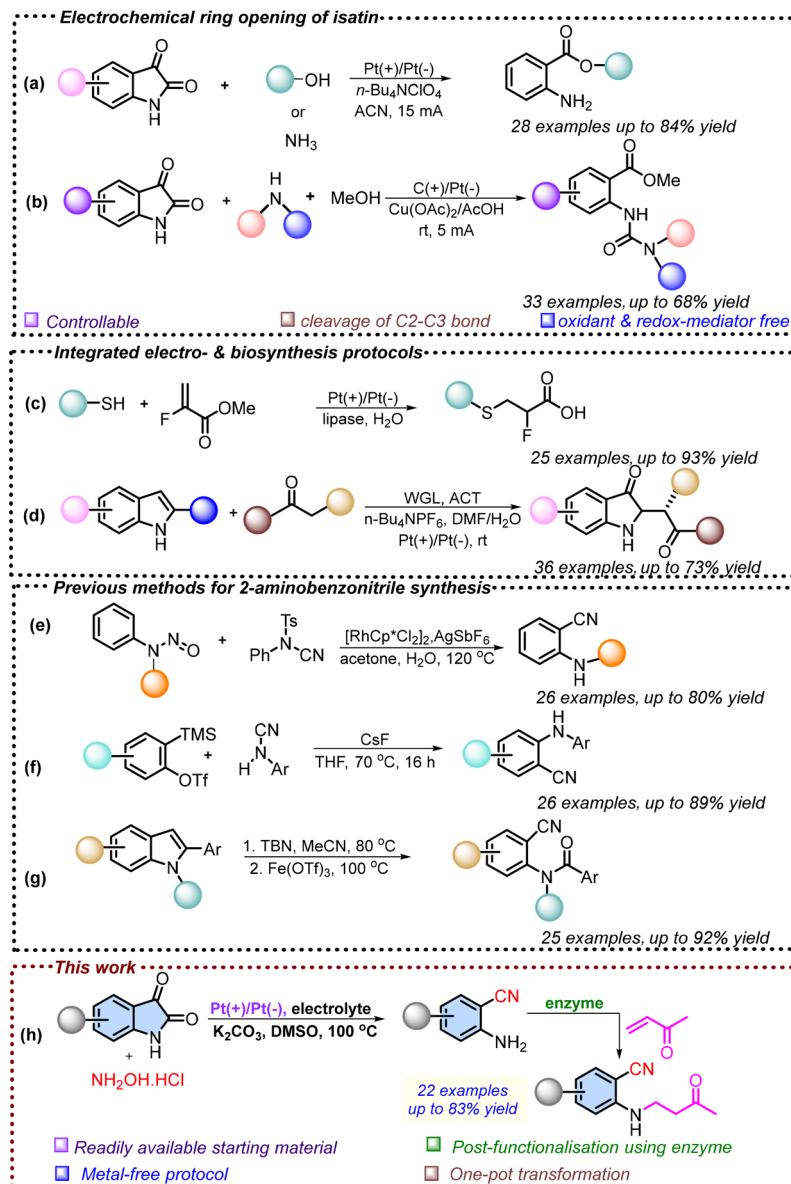
Numerous methods have been previously reported for cleaving the carbon–carbon bond in isatin; however, most of these approaches are limited by drawbacks such as the use of costly transition metal catalysts, stoichiometric chemical oxidants, and harsh reaction conditions.⁶

On the other hand, electrochemistry in organic synthesis has experienced remarkable growth and garnered widespread attention over the past decade, primarily due to its environmentally benign nature.⁷ Unlike conventional methods that rely on stoichiometric oxidants or reductants, electrochemical processes generate reactive intermediates directly *via* anodic oxidation or cathodic reduction, thereby minimizing hazardous reagents and improving the overall atom economy.⁸ Consequently, electrochemical methods have been successfully developed for the selective cleavage of carbon–carbon bonds in isatin.⁹ In this context, Wang *et al.* reported the electricity-driven cleavage of the C–C bond in isatin for the synthesis of anthranilic acid derivatives (Scheme 1a).¹⁰ Along with this, Liu *et al.* reported an efficient and convenient method for the ring opening of isatin using organic amines in an acidic buffer solution for the synthesis of methyl 2-ureidobenzoates (Scheme 1b).¹¹ Moreover, the integration of electrosynthesis with enzyme catalysis has emerged rapidly, reflecting a shift towards sustainable and efficient chemical transformations.¹² This merged system leverages the complementary strengths of both domains, where electrosynthesis provides a clean and green source of redox equivalents, and enzyme catalysis contributes exceptional selectivity and mild reaction conditions.¹³

^aDepartment of Chemistry and Biochemistry, Thapar Institute of Engineering and Technology, Patiala-147004, Punjab, India

^bDepartment of Chemistry, University of Lucknow, Lucknow-226007, Uttar Pradesh, India. E-mail: vikas.tyagi@thapar.edu





Scheme 1 Examples of oxidative ring opening of isatin and strategies to synthesize 2-aminobenzonitrile.

With respect to this, Tyagi *et al.* reported the synthesis of chiral sulphur-containing organofluorine acids in good yields using fluorine-based unsaturated alkenes and thiophenols by combining electrosynthesis and biocatalysis (Scheme 1c).^{13b} Additionally, Guan *et al.* reported the synthesis of 2,2-disubstituted 3-carbonyl indoles by integrating the non-natural catalytic activity of lipase with electrosynthesis, affording the products in good isolated yields as well as excellent enantio- and diastereoselectivities (Scheme 1d).^{13c}

Next, 2-aminobenzonitrile is an important moiety that has been used as a precursor for the synthesis of potent anti-inflammatory, antidiabetic, anti-HIV, antibacterial, and antiviral compounds, as shown in Fig. 1.¹⁴ Traditionally, 2-aminobenzonitriles have been synthesized *via* coupling or reduction of *o*-nitrobenzonitriles or related *o*-nitro derivatives.^{15–20} In

this context, Sun *et al.* reported a rhodium-catalyzed cyanation of aromatic C–H bonds, followed by denitrosation of nitrosoarylamines, using the nitroso group as a directing moiety. This strategy enabled the synthesis of 2-(alkylamino) benzonitriles, with *N*-cyano-*N*-phenyl-*p*-methylbenzenesulfonamide serving as the cyano source (Scheme 1e).²¹ In addition to this, Zeng *et al.* demonstrated an aminocyanation method for the synthesis of bifunctional aminobenzonitriles by direct addition of aryl cyanamides to arynes, which embeds both amino and cyano groups simultaneously (Scheme 1f).²² Furthermore, Mo *et al.* reported a one-pot *tert*-butyl nitrite (TBN)-mediated nitrosation followed by Fe-catalyzed cleavage of the carbon–carbon bond for the synthesis of 2-aminobenzonitriles in excellent yields, using 2-aryl indoles as the starting material (Scheme 1g).²³ While the aforementioned methods have been



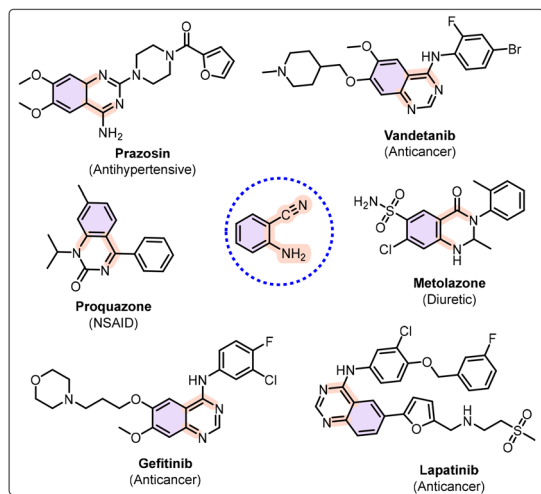


Fig. 1 Important pharmaceuticals containing 2-aminobenzonitrile.

successfully established for the synthesis of 2-aminobenzonitriles, they still have certain limitations, such as many of these approaches rely on starting materials that are not easily accessible, which restricts their broader applicability.²⁴ The frequent use of costly transition-metal catalysts further diminishes the practicality and economic feasibility of these protocols.^{25a,b} Therefore, there is a need to devise alternative strategies for the synthesis of 2-aminobenzonitrile derivatives that not only employ readily available and inexpensive starting materials but also utilize more affordable catalytic systems, thereby offering a more sustainable approach.

Inspired by the wide-ranging applications of 2-aminobenzonitriles and recognizing the limitations of conventional approaches, we propose an electricity-mediated, sustainable strategy for synthesizing 2-aminobenzonitrile derivatives from readily available isatins. Furthermore, by coupling the electrochemical step with enzyme catalysis, this approach enables an efficient two-step, one-pot synthesis of pharmaceutically significant β -amino carbonyl compounds (Scheme 1h).

Results and discussion

We began our study by establishing a model reaction in which isatin (**1a**) and hydroxylamine (**2a**) were electrolyzed using Pt/Pt electrodes and DMSO as the solvent at 120 °C. The reaction proceeded smoothly at a constant current of 10 mA in the presence of potassium iodide (KI) as the electrolyte and K_2CO_3 as the base, affording the desired product **3a** in 69% yield (entry 1, Table 1). This might be due to the limited solubility of KI in organic solvents, whereas *n*-Bu₄NI is highly soluble due to the lipophilic tetrabutylammonium cation, ensuring a uniform distribution of iodide ions throughout the reaction medium.^{25c} To further improve the yield, several reaction parameters were optimized, as summarized in Table 1. First, various electrolytes were screened. The use of tetrabutylammonium iodide (*n*-Bu₄NI) instead of KI significantly

Table 1 Optimisation of reaction conditions

Entry	Divergence from standard conditions	Yield ^b of 3a (%)
1	No change ^a	69
2	<i>n</i> -Bu ₄ NI instead of KI	82
3	KBr instead of KI	Nr
4	<i>n</i> -Bu ₄ NBr instead of KI	Nr
5	LiClO ₄ instead of KI	Trace
6	No current	Nr
7	5 mA instead of 10 mA	12
8	8 mA instead of 10 mA	67
9	15 mA instead of 10 mA	80
10	ACN instead of DMSO	Trace
11	DCE instead of DMSO	Nr
12	DMF instead of DMSO	19
13	THF instead of DMSO	23
14	TBAI (0.5 equiv.) instead of TBAI (1 equiv.)	49
15	TBAI (1.5 equiv.) instead of TBAI (1 equiv.)	87
16	TBAI (2 equiv.) instead of TBAI (1 equiv.)	79
17	Na ₂ CO ₃ instead of K ₂ CO ₃	34
18	Et ₃ N instead of K ₂ CO ₃	Nr
19	DBU instead of K ₂ CO ₃	Nr
20	No base	Nr
21	80 °C instead of 120 °C	55
22	100 °C instead of 120 °C	87
23	140 °C instead of 120 °C	79
24	0.5 equiv. of hydroxylamine instead of 2 equiv.	42
25	1 equiv. of hydroxylamine instead of 2 equiv.	69
26	1.5 equiv. of hydroxylamine instead of 2 equiv.	87
27	2.5 equiv. of hydroxylamine instead of 2 equiv.	85

^a Standard reaction conditions: isatin (**1a**) (20 mg, 1 equiv.), hydroxylamine (19 mg, 2 equiv.) (**2a**), KI (23 mg, 1 equiv.), K_2CO_3 (19 mg, 1 equiv.) in 1 mL of DMSO at a constant current of 10 mA in an undivided cell with Pt electrodes as the cathode and anode at 120 °C.

^b Yields were calculated using HPLC.

enhanced the yield to 82% (entry 2, Table 1). In contrast, when bromide salts such as KBr and *n*-Bu₄NBr were used in place of KI, no product formation was observed (entries 3 and 4, Table 1), while lithium perchlorate as an electrolyte afforded the product only in a trace amount (entry 5, Table 1). Importantly, no product (**3a**) formation was observed in the absence of current, highlighting the essential role of electricity in the process (entry 6, Table 1). Next, the effect of the current was examined. Decreasing the current from 10 mA to 5 mA led to a noticeable drop in yield (entries 7 and 8, Table 1), whereas increasing the current to 15 mA resulted in no significant improvement in the yield of the product (entry 9, Table 1). Furthermore, solvent screening revealed that replacing DMSO with acetonitrile (ACN) or 1,2-dichloroethane (DCE) gave no product, while DMF and THF provided significantly reduced yields compared to DMSO (entries 10–13, Table 1). Next, the electrolyte concentration was also optimized. Lowering the loading of TBAI from 1.0 to 0.5 equiv. decreased the yield of **3a** (entry 14, Table 1), whereas increasing it to 1.5 equiv. afforded **3a** in 87% yield (entry 15, Table 1). Moreover, a further

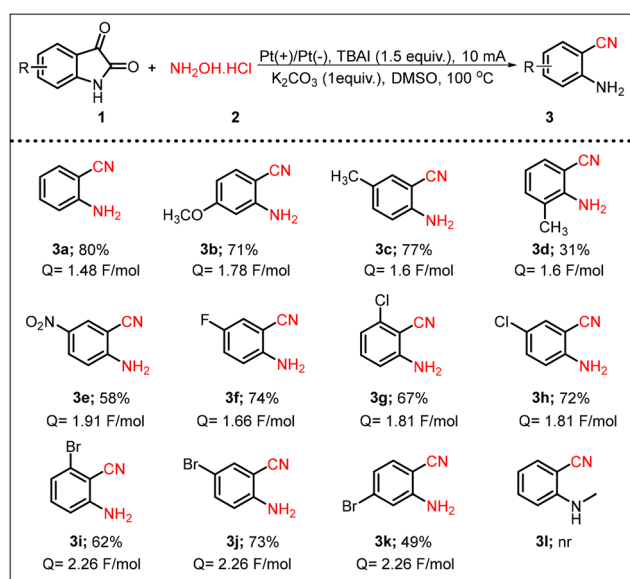


increase to 2.0 equiv. slightly reduced the yield of product **3a** (entry 16, Table 1). Moreover, optimization of the base showed that replacing K_2CO_3 with Na_2CO_3 decreased reaction efficiency, while organic bases such as Et_3N and DBU completely suppressed product formation (entries 17–19, Table 1). Notably, in the absence of a base, there was no product formation, confirming the requirement for a base in this protocol (entry 20, Table 1). Additionally, temperature studies revealed that lowering the reaction temperature to 80 °C decreased the yield to 55% (entry 21, Table 1), whereas operating at 100 °C yielded **3a** in up to 87% yield (entry 22, Table 1). However, increasing the temperature further to 140 °C led to a reduced yield of **3a** up to 79% (entry 23, Table 1). Finally, the stoichiometry of hydroxylamine was investigated. Reducing its amount to 0.5 equiv. or 1.0 equiv. decreased product (**3a**) formation (entries 24 and 25, Table 1), whereas 1.5 equiv. gave yields comparable to that for 2.0 equiv., establishing 1.5 equiv. as sufficient for optimal yield (entry 26, Table 1).

After optimizing the reaction conditions, the substrate scope of the electro-catalyzed reaction was thoroughly investigated, as shown in Scheme 2. First, we examined the influence of various electron-donating groups, such as $-OCH_3$ and $-CH_3$, at the C-5, C-6, and C-7 positions of isatin. Notably, the presence of an $-OCH_3$ group at the C-6 position provided a good yield, *i.e.*, 71% (**3b**, Scheme 2). In the case of a CH_3 group at the C-5 position of isatin, the product (**3c**) was obtained in an isolated yield of 77%, whereas a CH_3 group at the C-7 position led to a significantly lower yield of the corresponding product (**3d**). Next, we investigated the electron-withdrawing effect at the C-5 position, where an $-NO_2$ group present at this position

afforded the product in 58% yield (**3e**, Scheme 2). The influence of various halides, including $-F$, $-Cl$, and $-Br$, was examined at the C-4, C-5, and C-6 positions. It was observed that halide substitutions at the C-4 position resulted in lower yields (**3g** and **3i**, Scheme 2). In contrast, isatins having F, Cl, and Br at the C-5 position produced products in good yields (**3f**, **3h**, and **3j**, Scheme 2). Additionally, halide substitutions at the C-6 position resulted in lower product efficiency (**3k**, Scheme 2). However, no product formation was observed when *N*-methyl-substituted isatin was employed in the reaction (**3l**, Scheme 2).

In the second phase of our study, we conducted a reaction integrating electrochemical and α -amylase-catalyzed reaction conditions within a single vessel to synthesize a pharmaceutically relevant β -amino carbonyl compound (Scheme S1).²⁶ Conversely, the one-pot procedure produced the aza-Michael product in a notably low yield of only 12%. To improve the yield of the integrated protocol, the reaction conditions were modified. In this context, after completion of the electrochemical reaction, as confirmed by TLC, α -amylase (2 mg mL^{-1}), methyl vinyl ketone (1.5 equiv.), and water (1 mL) were added to the reaction mixture. The resulting mixture was stirred at 50 °C for 12 hours. Encouragingly, we obtained the aza-Michael product **4a** in an improved yield, *i.e.*, 45% (entry 1, Table 2). Furthermore, no reaction was observed when the enzyme concentration was reduced to 1 mg mL^{-1} (entry 2, Table 2). However, increasing the enzyme loading to 4 mg mL^{-1} and 6 mg mL^{-1} resulted in 56% and 52% isolated product yields, respectively (entries 3 and 4, Table 2). Additionally, the reaction medium was optimized for the enzymatic step by varying the amount of water. Reducing the volume of H_2O from 1 mL to 0.5 mL decreased the yield of **4a** to 39%. However, increasing the H_2O volume to 2 mL



Scheme 2 Substrate scope of electricity-mediated synthesis of 2-aminobenzonitrile. Reaction conditions: isatin (**1**) (100 mg, 1 equiv.), hydroxylamine (**2**) (71 mg, 1.5 equiv.), TBAI (377 mg, 1.5 equiv.), K_2CO_3 (95 mg, 1 equiv.) in 5 mL of DMSO at a constant current of 10 mA in an undivided cell with Pt electrodes as the cathode and anode at 100 °C.

Table 2 Optimisation of reaction conditions for the integrated protocol

Entry	Divergence from standard reaction conditions	Isolated yield of 4a (%)
1	No change	45
2	α -Amylase (1 mg mL^{-1})	No reaction
3	α -Amylase (4 mg mL^{-1})	56
4	α -Amylase (6 mg mL^{-1})	52
5	H_2O (0.5 mL)	39
6	H_2O (2 mL)	61
7	H_2O (2.5 mL)	60
8	MVK (2 equiv.)	68
9	MVK (2.5 equiv.)	76
10	MVK (3 equiv.)	74

Isatin (**1a**) (20 mg, 1 equiv.), hydroxylamine (14 mg, 1.5 equiv.) (**2a**), TBAI (75 mg, 1.5 equiv.), and K_2CO_3 (19 mg, 1 equiv.) in 1 mL of DMSO at a constant current of 10 mA in an undivided cell with Pt electrodes as the cathode and anode at 100 °C; after completion of the electrocatalytic step: α -amylase (2 mg mL^{-1}), methyl vinyl ketone (18 μ L, 1.5 equiv.), and 1 mL of water (v/v) at 50 °C, overnight, error = $\pm 4\%$ (reactions performed in triplicate).



improved the yield up to 61% (entry 6, Table 2). However, further increases beyond 2 mL did not significantly affect the yield of **4a** (entry 7, Table 2). Furthermore, increasing the amount of methyl vinyl ketone up to 2.5 equivalents improved the isolated yield of the product (entries 8 and 9, Table 2). However, further increasing the amount of methyl vinyl ketone, *i.e.*, 3.0 equivalents in comparison with isatin, did not significantly change the outcome of the reaction (entry 10, Table 2).

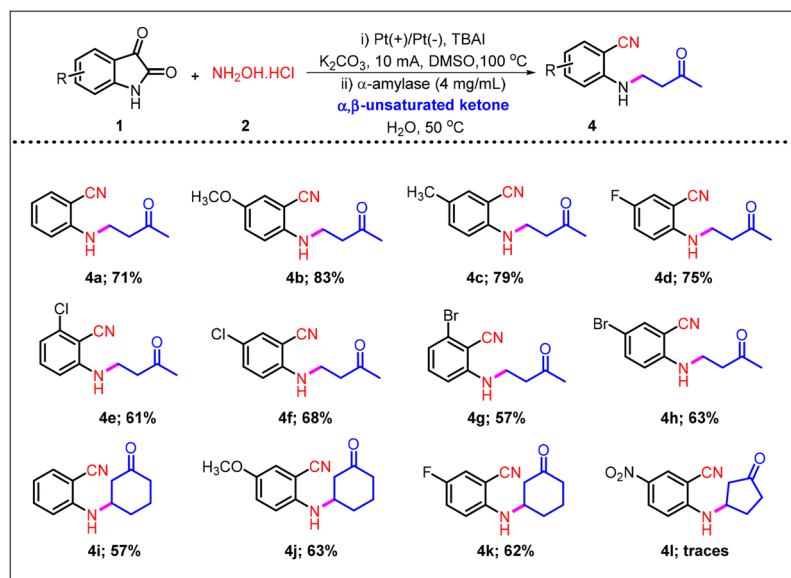
Standard reaction conditions

Furthermore, the substrate scope of the integrated protocol was thoroughly investigated under the optimal electro-biocatalytic reaction conditions, as shown in Scheme 3. In this context, electron-donating groups like methoxy and methyl facilitated the synthesis of the aza-Michael products in high yields (**4b–c**, Scheme 3). Additionally, halide substituents such as F, Cl, and Br at the C-4 and C-5 positions were well tolerated, affording the desired products in isolated yields ranging from 55% to 75% (**4d–h**, Scheme 3). Additionally, Michael acceptors such as cyclohexanone and cyclopentanone were investigated, along with differently substituted isatins, and as a result, the corresponding products were obtained in low to moderate yields (**4i–k**, Scheme 3). However, only a trace amount of the product was observed when cyclopentanone was employed in combination with 5-NO₂-substituted isatin (**4l**, Scheme 3).

To investigate the rate and influence of electricity and the enzyme at different reaction stages leading to the formation of **3a** and **4a**, we conducted a systematic study by designing a series of controlled reactions under optimized conditions, as

illustrated in Fig. 2. In the first experiment, substrates **1a** and **2a** were subjected to electrochemical conditions, resulting in the formation of **3a** within 2 hours. Along with the formation of **3a**, the consumption of isatin (**1a**) and the formation of isatin-3-oxime, an intermediate, were also monitored. The reaction showed complete consumption of isatin and formation of the corresponding isatin-3-oxime intermediate within 20 minutes. Subsequently, **3a** was treated under enzymatic conditions, facilitating its conversion to **4a** in 12 hours. Next, to validate the roles of electricity and the enzyme in the one-pot two-step protocol, we conducted different control experiments. First, an experiment was performed in the absence of electricity; however, the enzyme was still added to the reaction, and no formation of **3a** was observed, confirming the necessity of electricity for the formation of **3a**. Similarly, in the second experiment, electricity was employed without the addition of the enzyme, and no formation of **4a** took place, thereby verifying the essential role of the enzyme in the aza-Michael addition step. Finally, in the third experiment, where electricity and enzyme were both absent, neither **3a** nor **4a** was formed. These control experiments suggested that electricity plays a role in the formation of product **3a**, while the enzyme is necessary for the formation of **4a** *via* an aza-Michael addition reaction.

Next, based on the information available in the literature, we propose a plausible reaction mechanism for the electricity-mediated synthesis of 2-aminobenzonitrile, as illustrated in Scheme 4.^{10,27} The process begins with the condensation of substrates **1a** and **2a**, resulting in the formation of isatin-3-oxime (**I**).²⁸ At the cathode, water undergoes reduction, generating hydroxide ions. The electrogenerated hydroxide ion sub-



Scheme 3 Substrate scope of the integrated electro-biocatalytic synthesis of β -amino carbonyl compounds. Reaction conditions: (i) isatin (**1a**) (100 mg, 1 equiv.), hydroxyl amine (71 mg, 1.5 equiv.) (**2a**), TBAI (367 mg, 1.5 equiv.), and K₂CO₃ (95 mg, 1 equiv.) in 5 mL of DMSO at a constant current of 10 mA in an undivided cell with Pt electrodes as the cathode and anode at 100 °C; (ii) after completion of the electrocatalytic step: α -amylase (4 mg mL⁻¹), methyl vinyl ketone (150 μ L, 2.5 equiv.), 10 mL water (v/v) at 50 °C, overnight.



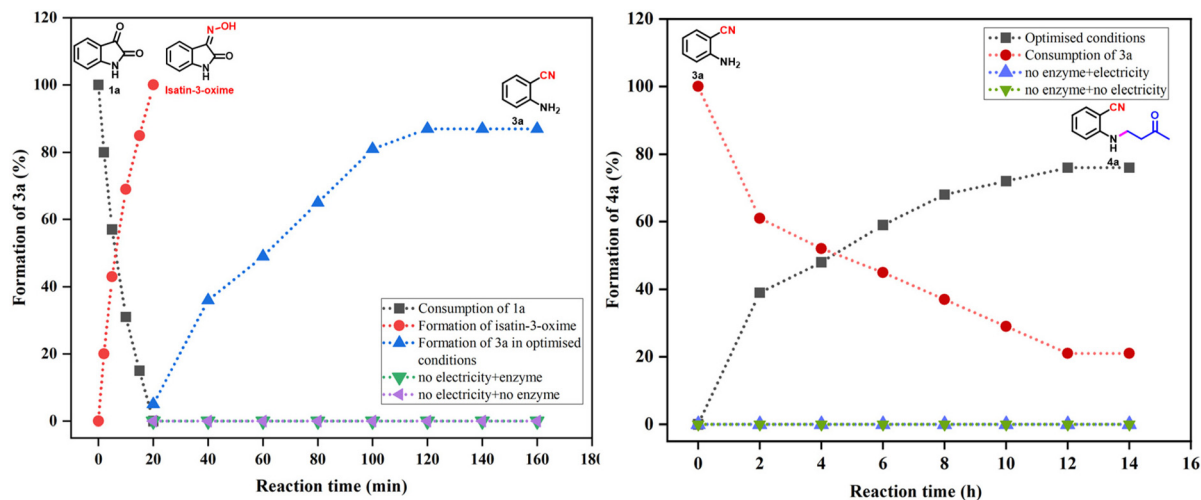
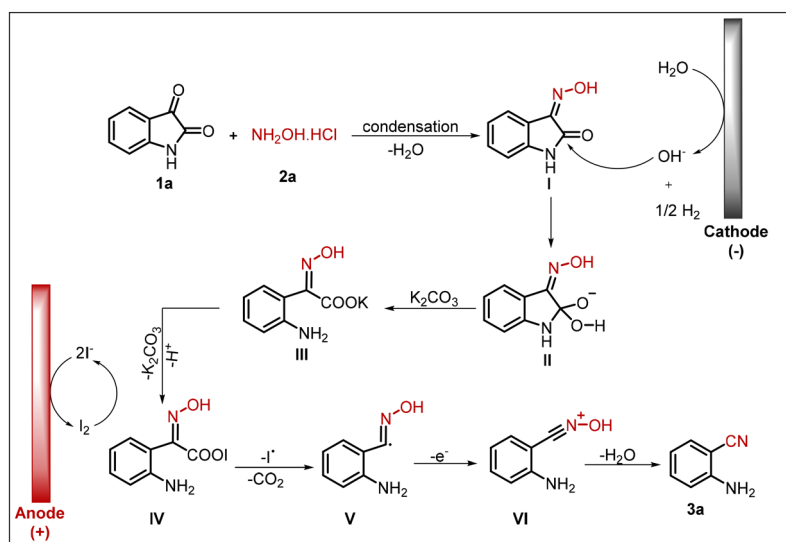


Fig. 2 (a) Role of electricity and enzyme in the formation of **3a** over time. (b) Role of electricity and enzyme in the formation of **4a** over time; optimised reaction conditions: (i) isatin (**1a**) (20 mg, 1 equiv.), hydroxylamine (14 mg, 1.5 equiv.) (**2a**), TBAI (75 mg, 1.5 equiv.), K_2CO_3 (19 mg, 1 equiv.) in 1 mL of DMSO at a constant current of 10 mA in an undivided cell having Pt electrodes as the cathode and the anode at 100 °C; (ii) after completion of the electrocatalytic step: α -amylase (4 mg mL⁻¹), methyl vinyl ketone (30 μ L, 2.5 equiv.), and 2 mL of water (v/v) at 50 °C, overnight.



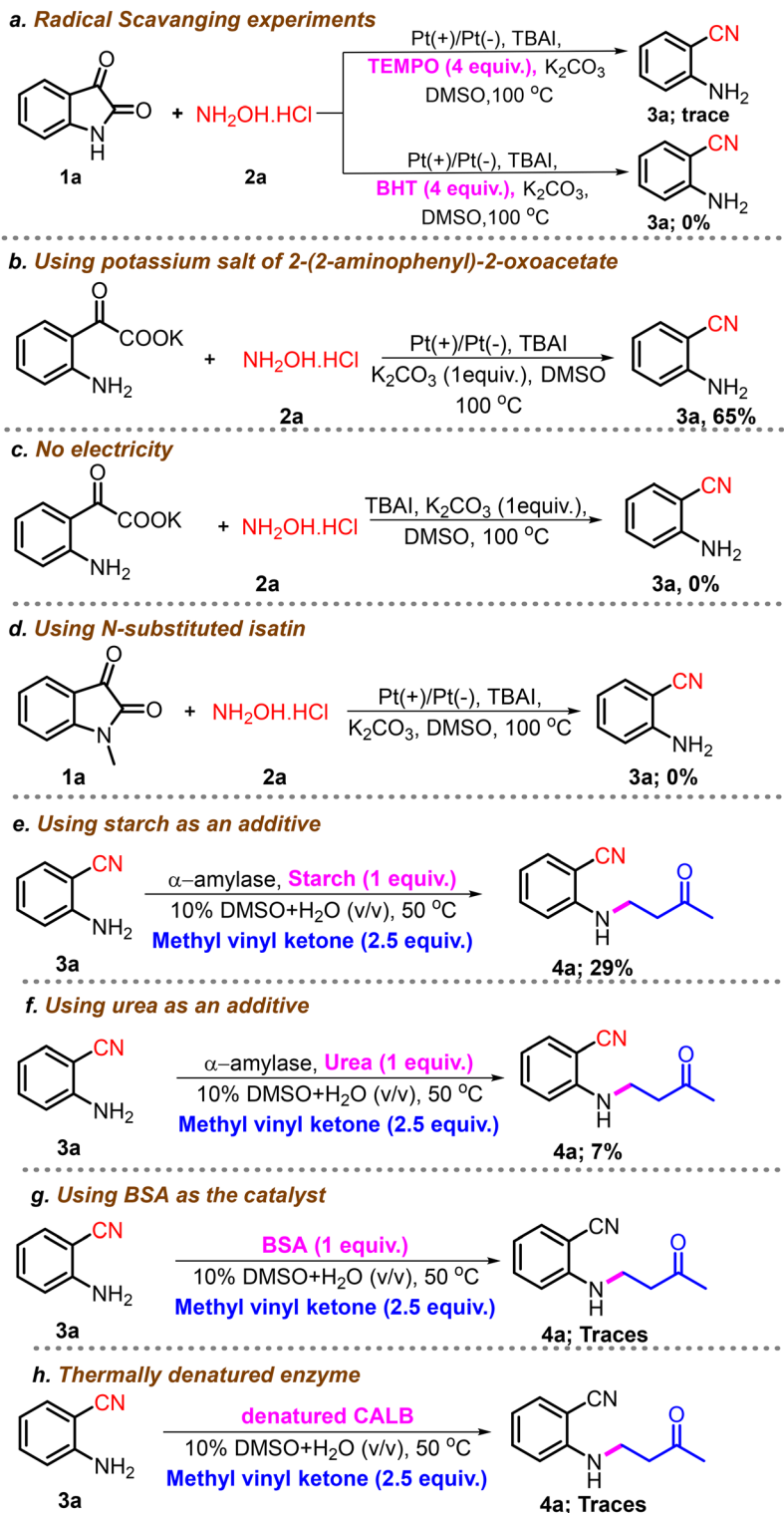
Scheme 4 Proposed mechanism for the electro-synthesis of 2-aminobenzonitriles.

sequently attacks intermediate **I**, producing intermediate **II**. Next, the base K_2CO_3 interacts with intermediate **II**, leading to electron redistribution and ring opening to yield intermediate **III**. Meanwhile, the iodide ion derived from tetrabutylammonium iodide (TBAI) is oxidised to molecular iodine (I_2), which reacts with intermediate **III**, and provides intermediate **IV**.¹⁰ This intermediate is unstable and readily eliminates an iodine radical with the concurrent release of carbon dioxide, affording intermediate **V**.²⁷ The carbon-centred radical in **V** then loses an electron to generate intermediate **VI**, which, upon dehydration, furnishes the desired product (**3a**).

Besides, to gain further insight into the proposed reaction mechanism, various control experiments were conducted.

First, radical-scavenging experiments were conducted in which 2,2,6,6-tetramethylpiperidin-1-oxyl (TEMPO) and butylated hydroxytoluene (BHT) were used as additives in the reaction. In the presence of TEMPO, product **3a** was obtained in only 5% yield, whereas no reaction was observed with BHT, thereby indicating the involvement of radical species in the reaction mechanism (Scheme 5a). Furthermore, the electricity-driven reaction was initiated with the sodium salt of 2-(2-aminophenyl)-2-oxoacetate and hydroxylamine hydrochloride, yielding the product **3a** in 65% yield (Scheme 5b). This experiment suggested the formation of intermediate **III** in the reaction, as determined by HRMS, and supports the proposed mechanistic pathway. Along with this, when the reaction of the sodium salt





Scheme 5 Control experiments.

of 2-(2-aminophenyl)-2-oxoacetate was performed in the absence of electricity, there was no formation of product 3a, which depicts the necessity of electricity for this reaction (Scheme 5c). Furthermore, when *N*-methyl-substituted isatin

was used in the electrochemical reaction, no formation of product 3a was observed (Scheme 5d). It was observed that no oxime formation occurred with *N*-methyl-substituted isatin, thereby suppressing the subsequent decarboxylation and electrochemical



reduction steps. In addition to the above experiments, control reactions were performed to verify the enzyme's role in the formation of the aza-Michael products. In this context, the first experiment was conducted by adding starch in an equimolar amount, and in the second experiment, urea was used in a 4.0 equivalent ratio corresponding to the enzyme. As a result, product **4a** was obtained in 29% and 7% isolated yields, respectively (Schemes 5e and f). Besides, when BSA was used as a catalyst in place of α -amylase, only a trace amount of **4a** was observed (Scheme 5g). Subsequently, to verify the role of the active site in catalyzing the reaction, the enzyme was thermally denatured, and the product **4a** was obtained only in a trace amount when denatured α -amylase was used as a catalyst (Scheme 5h).

Furthermore, a cyclic voltammetry (CV) study was conducted to investigate the underlying mechanism involved in the electrocatalysis of 2-aminobenzonitrile (Fig. 3).^{27,29,30} The CV profiles of potassium (*E*)-2-(2-aminophenyl)-2-(hydroxyimino)acetate (blue line), which is an intermediate, tetrabutylammonium iodide (TBAI, red line), and a blank sample (LiClO₄ in DMSO, black dotted line) were recorded using a platinum disc as the working electrode, a platinum wire as the counter electrode, and Ag/AgCl as the reference electrode. In the blank sample containing only the background electrolyte LiClO₄ and DMSO, no oxidation peak was observed, confirming the electrochemical inactivity of the solvent under the applied conditions. The cyclic voltammogram of TBAI revealed two characteristic anodic peaks at 0.535 V and 0.752 V vs. Ag/AgCl. These features are assigned to the stepwise redox processes involving oxidation of iodide ions to I₂ (I⁻ → I₂) followed by oxidation of triiodide species to iodine (I₃⁻ → I₂).²⁹ Notably, the CV of the mixture containing both TBAI and pot-

assium (*E*)-2-(2-aminophenyl)-2-(hydroxyimino)acetate exhibited an excessive oxidation potential peak at 1.378 V. During the reaction mechanism, potassium (*Z*)-2-(2-aminophenyl)-2-(hydroxyimino)acetate salt is formed, which undergoes halogenation to generate a hypiodite species due to *in situ* electro-generated I₂ and I₃⁻ in the presence of potassium salt.³⁰

Experimental

General information

All chemicals and solvents employed in this study were purchased from Sigma-Aldrich and used without further purification. α -Amylase from *Aspergillus oryzae* (≥ 150 U mg⁻¹, CAS no.: 232-588-1, product code: A9857), utilized for the functionalization of 2-aminobenzonitriles, was also procured from Sigma-Aldrich and used as received.

The electrochemical reactions were carried out using an OWON (P4305) instrument fitted with an undivided cell, a magnetic stirrer, and a set of platinum electrodes (2.5 cm length, 0.7 cm width and 0.05 mm thickness). Furthermore, the cyclic voltammetry study was performed using a DY2300 potentiostat instrument. The progress of the reaction was monitored using thin-layer chromatography (TLC, Silica 254G was coated on glass slides). The ¹H and ¹³C NMR characterisation of compounds was carried out using a JEOL or a Bruker spectrometer, at 400 MHz and 500 MHz for ¹H NMR and at 100 MHz and 125 MHz for ¹³C NMR. The spectra of samples were recorded in solvents CDCl₃ and *d*₆-DMSO using trimethyl silane as an internal standard (TMS). The chemical shift is denoted by δ (ppm) and the coupling constant is denoted by *J* (Hz). The chemical shift values of residual solvent peaks are as follows: for ¹H NMR, in CDCl₃ 7.26 ppm and in *d*₆-DMSO 2.50 ppm; for ¹³C NMR, in CDCl₃ 77.16 ppm and in *d*₆-DMSO 39.51 ppm. The abbreviations used for peak descriptions in NMR are as follows: brs, broad singlet; s, singlet; d, doublet; t, triplet; dd, doublet of doublets. The HRMS data of the compounds were characterised using a QTOF mass spectrometer (XEVO G2 XS) in ESI(+ve) mode.

General procedure for the synthesis of 2-aminobenzonitriles (3a–3k). In a reaction vial containing a magnetic bar, isatin (**1**) (100 mg, 1 equiv.), hydroxylamine hydrochloride (**2**) (71 mg, 1.5 equiv.), *n*Bu₄NI (376 mg, 1.5 equiv.) and base K₂CO₃ (95 mg, 1 equiv.) in 5 mL of DMSO were added, and the reaction mixture was stirred at 100 °C at a constant current of 10 mA in an undivided cell with platinum electrodes as the cathode and anode for 3 h. The progress of the reaction was monitored by thin-layer chromatography (TLC). Upon completion, the reaction mixture was extracted with ethyl acetate, and the organic layer was dried over anhydrous sodium sulphate. The solvent was removed under reduced pressure using a rotary evaporator, and the resulting residue was purified by column chromatography on silica gel (60–120 mesh) using hexane/ethyl acetate as the eluent to obtain the desired product.

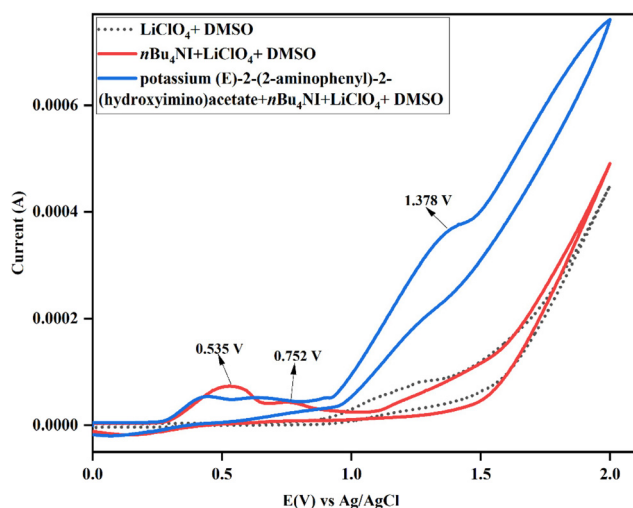


Fig. 3 Cyclic voltammetry using a Pt disc as the working electrode, Pt as the counter electrode & Ag/AgCl as the reference electrode; initial potential = zero volts, scan direction = 0 to +2 V (oxidative), room temperature. A cyclic voltammogram of potassium (*E*)-2-(2-aminophenyl)-2-(hydroxyimino)acetate (0.05 M) in DMSO with TBAI (0.01 M) and LiClO₄ (0.1 M) (the background electrolyte); scan rate 0.05 V s⁻¹, 0 to 2 V.



General procedure for the electro-biosynthesis of aza-Michael products (4a–4k). First, to a reaction vial containing a magnetic bar, isatin (**1**) (100 mg, 1 equiv.), hydroxylamine hydrochloride (**2**) (71 mg, 1.5 equiv.), *n*Bu₄NI (376 mg, 1.5 equiv.) and base K₂CO₃ (95 mg, 1 equiv.) in 5 mL of DMSO were added, and the mixture was stirred at 100 °C at a constant current of 10 mA in an undivided cell with platinum electrodes as the cathode and anode for 3 h. As indicated by TLC regarding the completion of the reaction, the reaction was cooled to room temperature, and methyl vinyl ketone (150 μL, 2.5 equiv.), α-amylase from *Aspergillus oryzae* (4 mg mL⁻¹), and 10 mL of H₂O were added. The above reaction mixture was stirred at 50 °C for 12 h. The reaction was monitored using TLC. After the reaction was complete, the mixture was extracted with ethyl acetate, and the organic layer was dried over anhydrous sodium sulphate and concentrated using a rotavapor. The residue was purified by column chromatography using 60–120 mesh silica gel as the stationary phase and hexane/ethyl acetate as the mobile phase.

Characterisation data of synthesized compounds

2-Aminobenzonitrile (3a). δ ¹H NMR (500 MHz, CDCl₃) δ 7.38 (dd, *J* = 8.2, 1.6 Hz, 1H), 7.35–7.30 (m, 1H), 6.76–6.70 (m, 2H), 4.41 (brs, 2H) ppm. ¹³C NMR (126 MHz, CDCl₃) δ 149.63, 134.06, 132.34, 118.02, 117.63, 115.14, 96.05 ppm. **HRMS (EI)** calculated for C₇H₆N₂ [M + H]⁺ 119.0609, found 119.0597.

2-Amino-4-methoxybenzonitrile (3b). δ ¹H NMR (300 MHz, CDCl₃) δ 7.31 (d, *J* = 8.7 Hz, 1H), 6.33 (dd, *J* = 8.7, 2.3 Hz, 1H), 6.23 (d, *J* = 2.4 Hz, 1H), 4.43 (brs, 2H), 3.81 (s, 3H) ppm. ¹³C NMR (76 MHz, CDCl₃) δ 164.21, 151.47, 133.88, 118.17, 105.83, 99.33, 88.68, 55.40 ppm. **HRMS (EI)** calculated for C₈H₈N₂O [M + H]⁺ 149.0715, found 149.0706.

2-Amino-5-methylbenzonitrile (3c). δ ¹H NMR (300 MHz, CDCl₃) δ 7.24–7.06 (m, 2H), 6.68 (d, *J* = 8.3 Hz, 1H), 4.29 (s, 2H), 2.24 (s, 3H) ppm. ¹³C NMR (76 MHz, CDCl₃) δ 147.48, 135.15, 131.94, 127.52, 117.85, 115.41, 95.99, 20.08 ppm. **HRMS (EI)** calculated for C₈H₈N₂ [M + H]⁺ 133.0766, found 133.0756.

2-Amino-3-methylbenzonitrile (3d). δ ¹H NMR (300 MHz, CDCl₃) δ 7.28 (d, *J* = 7.8 Hz, 1H), 7.23 (d, *J* = 7.4 Hz, 1H), 6.69 (t, *J* = 7.6 Hz, 1H), 4.41 (brs, 2H), 2.19 (s, 3H) ppm. ¹³C NMR (76 MHz, CDCl₃) δ 148.03, 135.27, 130.11, 122.62, 118.13, 117.57, 95.67, 17.42 ppm. **HRMS (EI)** calculated for C₈H₈N₂ [M + H]⁺ 133.0766, found 133.0756.

2-Amino-5-nitrobenzonitrile (3e). δ ¹H NMR (500 MHz, DMSO) δ 8.37 (d, *J* = 2.7 Hz, 1H), 8.12 (d, *J* = 2.7 Hz, 1H), 8.10 (d, *J* = 2.7 Hz, 1H), 7.47 (brs, 2H), 6.85 (d, *J* = 9.5 Hz, 1H) ppm. ¹³C NMR (126 MHz, DMSO) δ 135.75, 130.63, 129.39, 116.06, 114.97, 92.58 ppm. **HRMS (EI)** calculated for C₇H₅N₃O₂ [M + H]⁺ 164.0460, found 164.0472.

2-Amino-5-fluorobenzonitrile (3f). δ ¹H NMR (300 MHz, CDCl₃) δ 7.09 (td, *J* = 7.6, 2.9 Hz, 2H), 6.74–6.66 (m, 1H), 4.32 (brs, 2H) ppm. ¹³C NMR (76 MHz, CDCl₃) δ 156.15, 153.00, 146.51, 122.27 (d, ²*J*_{C-F} = 22.8 Hz), 117.76 (d, ²*J*_{C-F} = 25.1 Hz), 116.79 (d, ³*J*_{C-F} = 7.34 Hz), 96.08 ppm. **HRMS (EI)** calculated for C₇H₅FN₂ [M + H]⁺ 137.0515, found 137.0517.

2-Amino-6-chlorobenzonitrile (3g). δ ¹H NMR (500 MHz, DMSO) δ 7.25 (t, *J* = 8.4 Hz, 16.4 Hz, 1H), 6.74 (d, *J* = 7.6 Hz, 1H), 6.70 (s, 1H), 6.38 (brs, 2H) ppm. ¹³C NMR (126 MHz, DMSO) δ 153.63, 134.98, 134.43, 115.83, 115.34, 113.80, 93.85 ppm. **HRMS (EI)** calculated for C₇H₅ClN₂ [M + H]⁺ 153.0220, found 153.0212.

2-Amino-5-chlorobenzonitrile (3h). δ ¹H NMR (300 MHz, CDCl₃) δ 7.36 (d, *J* = 2.5 Hz, 1H), 7.29 (dd, *J* = 8.8, 2.4 Hz, 1H), 6.71 (d, *J* = 8.8 Hz, 1H), 4.49 (brs, 2H) ppm. ¹³C NMR (76 MHz, CDCl₃) δ 148.32, 134.35, 131.29, 122.37, 116.57, 96.95 ppm. **HRMS (EI)** calculated for C₇H₅ClN₂ [M + H]⁺ 153.0220, found 153.0217.

2-Amino-6-bromobenzonitrile (3i). δ ¹H NMR (300 MHz, CDCl₃) δ 7.15 (t, *J* = 8.1 Hz, 1H), 6.94 (d, *J* = 7.9 Hz, 1H), 6.67 (d, *J* = 9.4 Hz, 1H), 4.56 (brs, 2H) ppm. ¹³C NMR (76 MHz, CDCl₃) δ 151.53, 134.46, 125.08, 121.70, 116.28, 113.70, 99.59 ppm. **HRMS (EI)** calculated for C₇H₅BrN₂ [M + H]⁺ 196.9714, found 196.9713.

2-Amino-5-bromobenzonitrile (3j). δ ¹H NMR (300 MHz, CDCl₃) δ 7.49 (d, *J* = 2.4 Hz, 1H), 7.41 (dd, *J* = 8.8, 2.3 Hz, 1H), 6.66 (d, *J* = 8.8 Hz, 1H), 4.51 (brs, 2H) ppm. ¹³C NMR (76 MHz, CDCl₃) δ 148.70, 137.04, 134.16, 116.85, 116.31, 108.73, 97.54 ppm. **HRMS (EI)** calculated for C₇H₅BrN₂ [M + H]⁺ 196.9714, found 196.9709.

2-Amino-4-bromobenzonitrile (3k). δ ¹H NMR (300 MHz, CDCl₃) δ 7.28 (d, *J* = 4.0 Hz, 1H), 6.96 (d, *J* = 1.8 Hz, 1H), 6.89 (dd, *J* = 8.3, 1.8 Hz, 1H), 4.50 (s, 2H) ppm. ¹³C NMR (76 MHz, CDCl₃) δ 150.28, 133.40, 128.82, 121.39, 117.94, 116.98, 94.93 ppm. **HRMS (EI)** calculated for C₇H₅BrN₂ [M + H]⁺ 196.9714, found 196.9710.

2-((3-Oxobutyl)amino)benzonitrile (4a). δ ¹H NMR (500 MHz, CDCl₃) δ 7.40–7.34 (m, 2H), 6.71–6.60 (m, 2H), 4.82 (brs, 1H), 3.50 (q, *J* = 6.3 Hz, 2H), 2.80 (t, *J* = 6.5 Hz, 2H), 2.19 (s, 3H) ppm. ¹³C NMR (126 MHz, CDCl₃) δ 206.85, 149.94, 134.36, 132.66, 117.76, 116.67, 96.12, 42.51, 37.71, 30.33 ppm. **HRMS (EI)** calculated for C₁₁H₁₂N₂O 189.1028, found 189.1030.

5-Methoxy-2-((3-oxobutyl)amino)benzonitrile (4b). δ ¹H NMR (300 MHz, CDCl₃) δ 7.04 (d, *J* = 11.2 Hz, 1H), 6.91 (s, 1H), 6.67 (d, *J* = 8.0 Hz, 1H), 4.47 (brs, 1H), 3.76 (s, 3H), 3.47 (s, 2H), 2.81 (d, *J* = 7.1 Hz, 2H), 2.20 (s, 3H) ppm. ¹³C NMR (76 MHz, CDCl₃) δ 207.06, 150.81, 145.05, 122.43, 117.69, 115.98, 112.61, 96.25, 55.95, 42.63, 38.46, 30.42 ppm. **HRMS (EI)** calculated for C₁₂H₁₄N₂O₂ 219.1134, found 219.1132.

5-Methyl-2-((3-oxobutyl)amino)benzonitrile (4c). δ ¹H NMR (300 MHz, CDCl₃) δ 7.24 (d, *J* = 9.7 Hz, 2H), 6.65 (d, *J* = 8.4 Hz, 1H), 4.65 (brs, 1H), 3.52 (d, *J* = 6.4 Hz, 2H), 2.89–2.72 (m, 2H), 2.25 (d, *J* = 4.5 Hz, 6H) ppm. ¹³C NMR (76 MHz, CDCl₃) δ 206.99, 147.98, 135.28, 132.68, 126.24, 117.96, 110.82, 96.06, 42.56, 37.97, 30.42, 19.95 ppm. **HRMS (EI)** calculated for C₁₂H₁₄N₂O 203.1184, found 203.1187.

5-Fluoro-2-((3-oxobutyl)amino)benzonitrile (4d). δ ¹H NMR (300 MHz, CDCl₃) δ 7.17–7.02 (m, 2H), 6.67–6.55 (m, 1H), 4.69 (brs, 1H), 3.51–3.36 (m, 2H), 2.78 (td, *J* = 6.2, 2.4 Hz, 2H), 2.18 (s, 3H) ppm. ¹³C NMR (76 MHz, CDCl₃) δ 206.94, 155.31, 147.07, 122.10 (d, ²*J*_{C-F} = 21.9 Hz), 118.49 (d, ²*J*_{C-F} = 26.2 Hz), 116.71, 111.99 (d, ³*J*_{C-F} = 7.7 Hz), 95.98 (d, ³*J*_{C-F} = 7.7 Hz),



42.37, 38.24, 30.39 ppm. **HRMS (EI)** calculated for $C_{11}H_{11}FN_2O$ 207.0934, found 207.0939.

2-Chloro-6-((3-oxobutyl)amino)benzotrile (4e). 1H NMR (300 MHz, $CDCl_3$) δ 7.32–7.20 (m, 1H), 6.74–6.65 (m, 1H), 6.60–6.53 (m, 1H), 4.96 (brs, 1H), 3.53–3.44 (m, 2H), 2.80 (d, $J = 6.3$ Hz, 2H), 2.19 (s, 3H) ppm. ^{13}C NMR (76 MHz, $CDCl_3$) δ 206.79, 151.53, 137.19, 134.47, 117.31, 115.25, 108.57, 97.12, 42.34, 37.92, 30.45 ppm. **HRMS (EI)** calculated for $C_{11}H_{11}ClN_2O$ 223.0638, found 223.0632.

5-Chloro-2-((3-oxobutyl)amino)benzotrile (4f). 1H NMR (400 MHz, $CDCl_3$) δ 7.35 (d, $J = 7.1$ Hz, 2H), 6.65 (d, $J = 9.5$ Hz, 1H), 4.83 (brs, 1H), 3.50 (q, $J = 6.3$ Hz, 2H), 2.81 (t, $J = 6.4$ Hz, 2H), 2.22 (s, 3H) ppm. ^{13}C NMR (101 MHz, $CDCl_3$) δ 206.62, 148.58, 134.47, 131.91, 121.16, 116.52, 111.90, 97.14, 42.29, 37.90, 30.38 ppm. **HRMS (EI)** calculated for $C_{11}H_{11}ClN_2O$ 223.0638, 223.0634.

2-Bromo-6-((3-oxobutyl)amino)benzotrile (4g). 1H NMR (300 MHz, $CDCl_3$) 1H NMR (300 MHz, $CDCl_3$) δ 7.37–7.23 (m, 2H), 6.96 (d, $J = 7.7$ Hz, 1H), 6.69 (d, $J = 8.8$ Hz, 1H), 4.99 (brs, 1H), 3.56 (td, $J = 7.7, 3.5$ Hz, 2H), 2.87 (dt, $J = 8.7, 3.8$ Hz, 2H), 2.29 (s, 3H) ppm. ^{13}C NMR (76 MHz, $CDCl_3$) δ 206.64, 151.77, 134.69, 125.75, 120.58, 116.43, 109.05, 99.59, 42.42, 37.96, 30.50 ppm. **HRMS (EI)** calculated for $C_{11}H_{11}BrN_2O$ $[M + H]^+$ 267.0133, found 267.0130.

5-Bromo-2-((3-oxobutyl)amino)benzotrile (4h). 1H NMR (300 MHz, $CDCl_3$) δ 7.53–7.41 (m, 2H), 6.60 (d, $J = 13.6$ Hz, 1H), 4.87 (brs, 1H), 3.49 (dt, $J = 8.3, 4.1$ Hz, 2H), 2.82 (d, $J = 6.7$ Hz, 2H), 2.22 (s, 3H) ppm. ^{13}C NMR (76 MHz, $CDCl_3$) δ 206.66, 148.93, 137.19, 134.74, 116.41, 112.24, 107.43, 97.67, 42.25, 37.83, 30.38 ppm. **HRMS (EI)** calculated for $C_{11}H_{11}BrN_2O$ $[M + H]^+$ 267.0133, 267.0135.

(R)-2-((3-Oxocyclohexyl)amino)benzotrile (4i). 1H NMR (300 MHz, $CDCl_3$) δ 7.39 (dt, $J = 10.1, 5.1$ Hz, 2H), 6.74–6.57 (m, 2H), 4.50 (brs, 1H), 2.94–2.72 (m, 1H), 2.38 (tt, $J = 26.1, 13.0$ Hz, 4H), 2.13 (t, $J = 7.4$ Hz, 1H), 1.84–1.65 (m, 2H) ppm. ^{13}C NMR (76 MHz, $CDCl_3$) δ 208.45, 148.49, 134.49, 133.15, 117.26, 111.13, 96.32, 51.91, 48.19, 40.93, 31.48, 22.24 ppm. **HRMS (EI)** calculated for $C_{13}H_{14}N_2O$ $[M + H]^+$ 215.1184, found 215.1181.

(R)-5-Methoxy-2-((3-oxocyclohexyl)amino)benzotrile (4j). 1H NMR (300 MHz, $CDCl_3$) δ 7.08–6.80 (m, 2H), 6.66 (dd, $J = 17.6, 9.1$ Hz, 1H), 3.79 (brs, 1H), 3.72 (s, 3H), 2.83–2.76 (m, 1H), 2.44–2.27 (m, 2H), 2.10–1.96 (m, 3H), 1.72–1.59 (m, 3H) ppm. ^{13}C NMR (76 MHz, $CDCl_3$) δ 208.70, 151.66, 144.31, 122.77, 117.18, 116.02, 114.65, 113.35, 96.57, 55.99, 52.80, 48.36, 40.92, 31.56, 22.20 ppm. **HRMS (EI)** calculated for $C_{14}H_{16}N_2O_2$ $[M + H]^+$ 245.1290, found 245.1290.

(R)-5-Fluoro-2-((3-oxocyclohexyl)amino)benzotrile (4k). 1H NMR (300 MHz, $CDCl_3$) 1H δ 7.19–7.10 (m, 2H), 6.62 (dd, $J = 9.0, 4.2$ Hz, 1H), 4.36 (brs, 1H), 2.82 (ddt, $J = 13.8, 4.0, 1.9$ Hz, 1H), 2.67–2.12 (m, 4H), 2.28–2.01 (m, 2H), 1.82–1.34 (m, 2H) ppm. ^{13}C NMR (76 MHz, $CDCl_3$) δ 208.30, 152.42, 145.49, 122.34 (d, $^2J_{C-F} = 23.00$ Hz), 118.77 (d, $^2J_{C-F} = 25.20$ Hz), 112.59 (d, $^3J_{C-F} = 7.47$ Hz), 96.37 (d, $^3J_{C-F} = 9.14$ Hz), 52.41, 48.18, 40.92, 31.56, 22.23 ppm. **HRMS (EI)** calculated for $[M + H]^+$ 233.1090, found 233.1088.

Conclusion

In summary, we have developed an electricity-mediated, sustainable protocol for the efficient synthesis of 2-aminobenzonitriles from isatins and hydroxylamine as starting materials. This strategy overcomes the limitations of previously reported methods that often require harsh reaction conditions, metal catalysts, or costly substrates. A range of substituted 2-aminobenzonitriles were obtained in good yields directly from the corresponding substituted isatins. Furthermore, the electrochemically synthesized 2-aminobenzonitriles were successfully functionalized in a one-pot process by integrating electrochemical synthesis with α -amylase-catalyzed aza-Michael addition, affording clinically valuable β -amino carbonyl compounds. Furthermore, control experiments and cyclic voltammetry studies were conducted to gain mechanistic insight into the integrated protocol. Overall, this protocol highlights the potential of electrochemically driven C–C bond cleavage in isatin chemistry.

Author contributions

Kirti Singh: writing – original draft, methodology, and investigation. Shashi Pandey: data characterisation and compilation of data. Vikas Tyagi: writing – original draft, project administration, investigation, and conceptualisation.

Conflicts of interest

The authors declare no conflicts of interest.

Data availability

The data supporting this article have been included as part of the supplementary information (SI). Supplementary information is available. See DOI: <https://doi.org/10.1039/d5ob01983d>.

Acknowledgements

Financial support from the Department of Biotechnology, Ministry of Science and Technology, Government of India (BT/PR55062/BSA/33/294/2024), and the DST/INSPIRE Fellowship/2020/IF200048 is greatly acknowledged. The authors are also grateful to the Department of Science and Technology Grant (SR/FST/CS-II/2018/69) at the Department of Chemistry and Biochemistry, Thapar Institute of Engineering and Technology, Patiala, for providing the HRMS data.

References

- (a) Y. F. Liang, M. Bilal, L. Y. Tang, T. Z. Wang, Y. Q. Guan, Z. Cheng, M. Zhu, J. Wei and N. Jiao, Carbon–carbon bond



- cleavage for late-stage functionalization, *Chem. Rev.*, 2023, **123**, 12313–12370; (b) F. Chen, T. Wang and N. Jiao, Recent advances in transition-metal-catalyzed functionalization of unstrained carbon–carbon bonds, *Chem. Rev.*, 2014, **114**, 8613–8661; (c) D. Ravelli, S. Protti and M. Fagnoni, Carbon–carbon bond forming reactions via photogenerated intermediates, *Chem. Rev.*, 2016, **116**, 9850–9913; (d) P. Sivaguru, Z. Wang, G. Zaroni and X. Bi, Cleavage of carbon–carbon bonds by radical reactions, *Chem. Soc. Rev.*, 2019, **48**, 2615–2656; (e) I. Marek, A. Masarwa, P. O. Delaye and M. Leibelng, Selective carbon–carbon bond cleavage for the stereoselective synthesis of acyclic systems, *Angew. Chem., Int. Ed.*, 2015, **54**, 414–429.
- 2 (a) P. Nath, A. Mukherjee, S. Mukherjee, S. Banerjee, S. Das and S. Banerjee, Isatin: a scaffold with immense biodiversity, *Mini-Rev. Med. Chem.*, 2021, **21**, 1096–1112; (b) A. Mondal, A brief review depending on the chemistry of isatin in single pot technique towards the construction of significant and valuable heterocyclic scaffolds, *Lett. Org. Chem.*, 2024, **21**, 929–957; (c) P. Yadav, S. Berry and A. Bhalla, Chemical methods for the construction of spirocyclic β -lactams and their biological importance, *Synthesis*, 2025, 251–274; (d) D. Karati, An insight into isatin and its hybrid scaffolds as anti-cancer agents: an explicative review, *Discov. Chem.*, 2024, **1**, 66; (e) I. M. Andrade, E. D. O. Lima Filho, C. F. Valadão, L. D. S. Forezi and F. de C. da Silva, Recent advances in isatin–thiazole hybrids: synthesis, structural design, and biological application, *Chem. Biodiversity*, 2025, e01989.
- 3 (a) R. Kakkar, Isatin and its derivatives: a survey of recent syntheses, reactions, and applications, *MedChemComm*, 2019, **10**, 351–368; (b) R. E. Ferraz de Paiva, E. G. Vieira, D. Rodrigues da Silva, C. A. Wegermann and A. M. Costa Ferreira, Anticancer compounds based on isatin-derivatives: strategies to ameliorate selectivity and efficiency, *Front. Mol. Biosci.*, 2021, **7**, 627272; (c) R. S. Cheke, V. M. Patil, S. D. Firke, J. P. Ambhore, I. A. Ansari, H. M. Patel, S. D. Shinde, V. R. Pasupuleti, M. I. Hassan, M. Adnan and A. Kadri, Therapeutic outcomes of isatin and its derivatives against multiple diseases: recent developments in drug discovery, *Pharmaceuticals*, 2022, **15**, 272; (d) S. Bugalia, Y. Dhayal, H. Sachdeva, S. Kumari, K. Atal, U. Phageria, P. Saini and O. P. Gurjar, Review on isatin—a remarkable scaffold for designing potential therapeutic complexes and its macrocyclic complexes with transition metals, *J. Inorg. Organomet. Polym. Mater.*, 2023, **33**, 1782–1801; (e) V. A. Shu, D. B. Eni and F. Ntie-Kang, A survey of isatin hybrids and their biological properties, *Mol. Divers.*, 2025, **29**, 1737–1760.
- 4 (a) C. Xu, F. C. Jia, Q. Cai, D. K. Li, Z. W. Zhou and A. X. Wu, Intramolecular decarboxylative coupling as the key step in copper-catalyzed domino reaction: facile access to 2-(1,3,4-oxadiazol-2-yl)aniline derivatives, *Chem. Commun.*, 2015, **51**, 6629–6632; (b) Y. Ma, Y. Zhu, D. Zhang, Y. Meng, T. Tang, K. Wang, J. Ma, J. Wang and P. Sun, Eco-friendly decarboxylative cyclization in water: practical access to the anti-malarial 4-quinolones, *Green Chem.*, 2019, **21**, 478–482; (c) F. C. Jia, Z. W. Zhou, C. Xu, Y. D. Wu and A. X. Wu, Divergent synthesis of quinazolin-4(3H)-ones and tryptanthrins enabled by a tert-butyl hydroperoxide/ K_3PO_4 -promoted oxidative cyclization of isatins at room temperature, *Org. Lett.*, 2016, **18**, 2942–2945; (d) F. C. Jia, T. Z. Chen and X. Q. Hu, TFA/TBHP-promoted oxidative cyclisation for the construction of tetracyclic quinazolinones and rutaecarpine, *Org. Chem. Front.*, 2020, **7**, 1635–1639; (e) A. H. Kalbandhe, A. C. Kavale, P. B. Thorat and N. N. Karade, Oxidative cleavage of the C2–C3 bond in isatin using (diacetoxyiodo)benzene: a facile synthesis of carbamates of alkyl anthranilates, *Synlett*, 2016, 763–768.
- 5 (a) N. U. A. Mohsin and M. Irfan, Selective cyclooxygenase-2 inhibitors: A review of recent chemical scaffolds with promising anti-inflammatory and COX-2 inhibitory activities, *Med. Chem. Res.*, 2020, **29**(5), 809–830; (b) L. D. Brown, A. S. Girgis, S. Patel, N. Samir, M. F. Said, A. T. Baidya, R. Kumar, J. Moore, A. Khadanga, R. Sakhuja and S. S. Panda, Novel isatin conjugates endowed with analgesic and anti-inflammatory properties: design, synthesis and biological evaluation, *Future Med. Chem.*, 2025, **17**, 59–73; (c) L. M. Zhou, R. Y. Qu and G. F. Yang, An overview of spirooxindole as a promising scaffold for novel drug discovery, *Expert Opin. Drug Discovery*, 2020, **15**, 603–625; (d) S. Chahal, P. Rani, Kiran, J. Sindhu, G. Joshi, A. Ganesan, S. Kalyanamoorthy, Mayank, P. Kumar, R. Singh and A. Negi, Design and development of COX-II inhibitors: current scenario and future perspective, *ACS Omega*, 2023, **8**, 17446–17498; (e) R. A. Menezes and K. S. Bhat, Synthetic aspects, structural insights and pharmacological potential of pyrazole derivatives: an overview, *Discover Appl. Sci.*, 2025, **7**, 137; (f) S. Mukherjee and M. Pal, Medicinal chemistry of quinolines as emerging anti-inflammatory agents: an overview, *Curr. Med. Chem.*, 2013, **20**, 4386–4410.
- 6 (a) P. V. Gandhi, S. R. Burande, M. S. Charde and R. D. Chakole, A review on isatin and its derivatives: synthesis, reactions and applications, *J. Adv. Sci. Res.*, 2021, **12**(04), 1–11; (b) A. Zafar, M. A. Iqbal, G. Iram, U. S. Shoukat, F. Jamil, M. Saleem, M. Yousif, Z. ul Abidin and M. Asad, Advances in organocatalyzed synthesis of organic compounds, *RSC Adv.*, 2024, **14**, 20365–20389; (c) C. Pradhan and B. Punji, Advancement in the C–H bond alkylation of (hetero)arenes catalyzed by the most abundant transition metal–iron, *Org. Chem. Front.*, 2024, **11**, 2397–2417.
- 7 (a) Y. H. Budnikova, E. L. Dolengovski, M. V. Tarasov and T. V. Gryaznova, Electrochemistry in organics: a powerful tool for “green” synthesis, *J. Solid State Electrochem.*, 2024, **28**, 659–676; (b) T. H. Meyer, I. Choi, C. Tian and L. Ackermann, Powering the future: how can electrochemistry make a difference in organic synthesis?, *Chem*, 2020, **6**, 2484–2496; (c) Q. Jing and K. D. Moeller, From molecules to molecular surfaces: exploiting the interplay between organic synthesis and electrochemistry, *Acc. Chem.*



- Res.*, 2019, **53**, 135–143; (d) T. Ali, H. Wang, W. Iqbal, T. Bashir, R. Shah and Y. Hu, Electro-synthesis of organic compounds with heterogeneous catalysis, *Adv. Sci.*, 2023, **10**, 2205077; (e) C. Ma, J. F. Guo, S. S. Xu and T. S. Mei, Recent advances in asymmetric organometallic electrochemical synthesis (AOES), *Acc. Chem. Res.*, 2025, **58**, 399–414; (f) Z. Shi, C. Y. Wen, L. X. Yang, J. Li and X. Sun, Recent progress in electrochemical rearrangement reactions, *Org. Chem. Front.*, 2025, **12**, 2499–2524.
- 8 (a) N. Li, R. Sitdikov, A. P. Kale, J. Steverlynck, B. Li and M. Rueping, A review of recent advances in electrochemical and photoelectrochemical late-stage functionalization classified by anodic oxidation, cathodic reduction, and paired electrolysis, *Beilstein J. Org. Chem.*, 2024, **20**, 2500–2566; (b) J. Liu, L. Lu, D. Wood and S. Lin, New redox strategies in organic synthesis by means of electrochemistry and photochemistry, *ACS Cent. Sci.*, 2020, **6**, 1317–1340; (c) L. F. Novaes, J. Liu, Y. Shen, L. Lu, J. M. Meinhardt and S. Lin, Electrocatalysis as an enabling technology for organic synthesis, *Chem. Soc. Rev.*, 2021, **50**, 7941–8002; (d) X. Cheng, A. Lei, T. S. Mei, H. C. Xu, K. Xu and C. Zeng, Recent applications of homogeneous catalysis in electrochemical organic synthesis, *CCS Chem.*, 2022, **4**, 1120–1152; (e) J. Q. Lu, Y. K. Wang, T. McCallum and N. Fu, Harnessing radical chemistry via electrochemical transition metal catalysis, *iScience*, 2020, **23**, 101796; (f) P. Li, Y. Wang, H. Zhao and Y. Qiu, Electroreductive cross-coupling reactions: carboxylation, deuteration and alkylation, *Acc. Chem. Res.*, 2024, **58**, 113–129; (g) C.-Y. Sun, T.-J. Lin, Y.-Y. Chen, H.-L. Li and C.-W. Chiang, Synergistic photoredox and electrochemical catalysis in organic synthesis and late-stage functionalizations, *ChemCatChem*, 2024, **16**, e202301537; (h) Y. Chen, S. Ji, C. Chen, Q. Peng, D. Wang and Y. Li, Single-atom catalysts: synthetic strategies and electrochemical applications, *Joule*, 2018, **2**, 1242–1264; (i) W. Guo, K. Zhang, Z. Liang, R. Zou and Q. Xu, Electrochemical nitrogen fixation and utilization: theories, advanced catalyst materials and system design, *Chem. Soc. Rev.*, 2019, **48**, 5658–5716; (j) M. Zhang, Q. Shi, X. Song, H. Wang and Z. Bian, Recent electrochemical methods in electrochemical degradation of halogenated organics: a review, *Environ. Sci. Pollut. Res.*, 2019, **26**, 10457–10486; (k) B. P. Chaplin, The prospect of electrochemical technologies advancing worldwide water treatment, *Acc. Chem. Res.*, 2019, **52**, 596–604.
- 9 (a) S. H. Shi, Y. Liang and N. Jiao, Electrochemical oxidation induced selective C–C bond cleavage, *Chem. Rev.*, 2020, **121**, 485–505; (b) Y. Adeli, K. Huang, Y. Liang, Y. Jiang, J. Liu, S. Song, C.-C. Zeng and N. Jiao, Electrochemically oxidative C–C bond cleavage of alkylarenes for aniline synthesis, *ACS Catal.*, 2019, **9**, 2063–2067; (c) S. Zhang, L. Li, J. Li, J. Shi, K. Xu, W. Gao, L. Zong, G. Li and M. Findlater, Electrochemical arylation of aldehydes, ketones, and alcohols: from cathodic reduction to convergent paired electrolysis, *Angew. Chem.*, 2021, **133**, 7351–7358.
- 10 P. Qian, J. Liu, Y. Zhang and Z. Wang, Tunable electro-synthesis of anthranilic acid derivatives via a C–C bond cleavage of isatins, *J. Org. Chem.*, 2021, **86**, 16008–16015.
- 11 M. Zhao, J. Fu, Y. Sang, Z. Wang, W. Liu and C. Chen, Electrosynthesis of methyl 2-ureidobenzoates via a C2–C3 bond cleavage of isatins, *Tetrahedron*, 2023, **137**, 133383.
- 12 (a) C. Ma, Y. Wang, K. Guo, R. Wu and Z. Zhu, Enzymatic electro-synthesis system based on multi-enzyme catalysis or coupled with microbial transformation, *Catal. Sci. Technol.*, 2025, **15**, 1390–1405; (b) L. Liu and D. Pant, Integrative electrochemical and biological catalysis for the mild and efficient utilization of renewable electricity and carbon resources, *Sustainable Energy Fuels*, 2024, **8**, 460–480; (c) H. Chen, O. Simoska, K. Lim, M. Grattieri, M. Yuan, F. Dong, Y. S. Lee, K. Beaver, S. Weliwatte, E. M. Gaffney and S. D. Minter, Fundamentals, applications, and future directions of bioelectrocatalysis, *Chem. Rev.*, 2020, **120**, 12903–12993; (d) R. Wu, F. Li, X. Cui, Z. Li, C. Ma, H. Jiang, L. Zhang, Y. H. P. J. Zhang, T. Zhao, Y. Zhang and Y. Li, Enzymatic electro-synthesis of glycine from CO₂ and NH₃, *Angew. Chem., Int. Ed.*, 2023, **62**, e202218387.
- 13 (a) K. Singh and V. Tyagi, Combining the nonnatural activity of lipase and electrocatalysis in one pot: sustainable and regioselective synthesis of C-3 alkylated oxindoles, *ChemCatChem*, 2025, **17**, e202401182; (b) P. Kaur and V. Tyagi, Merging electro-synthesis and biocatalysis to access sulfur-based chiral α -fluorinated carboxylic acids, *J. Org. Chem.*, 2025, **90**, 5378–5392; (c) C. J. Long, H. Cao, B. K. Zhao, Y. F. Tan, Y. H. He, C. S. Huang and Z. Guan, Merging the non-natural catalytic activity of lipase and electro-synthesis: asymmetric oxidative cross-coupling of secondary amines with ketones, *Angew. Chem.*, 2022, **134**, e202203666; (d) I. Peñafiel, R. A. Dryfe, N. J. Turner and M. F. Greaney, Integrated electro-biocatalysis for amine alkylation with alcohols, *ChemCatChem*, 2021, **13**, 864–867.
- 14 (a) A. A. H. Abdel-Rahman, E. M. El-Ganzoury, I. F. Zeid, E. M. Zayed and W. A. El-Sayed, Quinazolines linked to sugar derivatives as nucleoside analogs: synthesis and biological aspects, *Egypt. J. Chem.*, 2024, **67**, 209–223; (b) M. Benabdallah, O. Talhi, F. Nouali, N. Choukchou-Braham, K. Bachari and A. Silva, Advances in spirocyclic hybrids: chemistry and medicinal actions, *Curr. Med. Chem.*, 2018, **25**, 3748–3767; (c) P. Yadav and A. Bhalla, Recent advances in green synthesis of functionalized quinolines of medicinal impact (2018–present), *ChemistrySelect*, 2022, **7**, e202201721; (d) W. Spillane and J. B. Malaubier, Sulfamic acid and its N- and O-substituted derivatives, *Chem. Rev.*, 2014, **114**, 2507–2586; (e) V. T. Nguyen, D. P. Tran, T. T. Nguyen, K. D. Nguyen and H. V. Le, An efficient and green synthesis of 2-phenylquinazolin-4(3H)-ones via t-BuONa-mediated oxidative condensation of 2-aminobenzamides and benzyl alcohols under solvent- and transition metal-free conditions, *Green Process. Synth.*, 2023, **12**, 20228148.
- 15 (a) X. J. Yang, B. Chen, L. Q. Zheng, L. Z. Wu and C. H. Tung, Highly efficient and selective photocatalytic



- hydrogenation of functionalized nitrobenzenes, *Green Chem.*, 2014, **16**, 1082–1086; (b) M. Nabi, K. Sharma, R. S. Wandre and A. B. Gade, One-pot oximation–Beckmann rearrangement under mild, aqueous micellar conditions, *Green Chem.*, 2025, **27**, 5332–5339.
- 16 H. Goksu, S. F. Ho, O. Metin, K. Korkmaz, A. Mendoza Garcia, M. S. Gultekin and S. Sun, Tandem dehydrogenation of ammonia borane and hydrogenation of nitro/nitrile compounds catalyzed by graphene-supported NiPd alloy nanoparticles, *ACS Catal.*, 2014, **4**, 1777–1782.
- 17 K. Kim and S. H. Hong, Photoinduced copper(I)-catalyzed cyanation of aromatic halides at room temperature, *Adv. Synth. Catal.*, 2017, **359**, 2345–2351.
- 18 B. Majhi and B. C. Ranu, Palladium-catalyzed norbornene-mediated tandem ortho-C–H amination/ipso-C–I cyanation of iodoarenes: regiospecific synthesis of 2-aminobenzonitrile, *Org. Lett.*, 2016, **18**, 4162–4165.
- 19 G. Dou and D. Shi, Efficient and convenient synthesis of indazol-3(2H)-ones and 2-aminobenzonitriles, *J. Comb. Chem.*, 2009, **11**, 1073–1077.
- 20 Z. Wei, J. Wang, S. Mao, D. Su, H. Jin, Y. Wang, F. Xu, H. Li and Y. Wang, In situ-generated Co⁰–Co₃O₄/N-doped carbon nanotubes hybrids as efficient and chemoselective catalysts for hydrogenation of nitroarenes, *ACS Catal.*, 2015, **5**, 4783–4789.
- 21 J. Dong, Z. Wu, Z. Liu, P. Liu and P. Sun, Rhodium(III)-catalyzed direct cyanation of aromatic C–H bond to form 2-(alkylamino)benzonitriles using N-nitroso as directing group, *J. Org. Chem.*, 2015, **80**, 12588–12593.
- 22 B. Rao and X. Zeng, Aminocyanation by the addition of N–CN bonds to arynes: chemoselective synthesis of 1,2-bifunctional aminobenzonitriles, *Org. Lett.*, 2014, **16**, 314–317.
- 23 W. L. Chen, S. Y. Wu, X. L. Mo, L. X. Wei, C. Liang and D. L. Mo, Synthesis of 2-aminobenzonitriles through nitrosation reaction and sequential iron(III)-catalyzed C–C bond cleavage of 2-arylindoles, *Org. Lett.*, 2018, **20**, 3527–3530.
- 24 (a) Q. Zhang and X. Jin, Recent advances in the fixation of CO₂ to form N-containing heterocyclic compounds, *Chem. – Eur. J.*, 2025, **31**, e202500933; (b) W. Huang, D. He, H. Jiang and W. Wu, Recent advances in the transformation of nitriles into diverse N-heterocycles, *Chem. Soc. Rev.*, 2025, **54**, 10724–10795; (c) H. Li, H. Guo, Z. Fang, T. M. Aida and R. L. Smith, Cycloamination strategies for renewable N-heterocycles, *Green Chem.*, 2020, **22**, 582–611.
- 25 (a) R. Tamatam, S. H. Kim and D. Shin, Transition-metal-catalyzed synthesis of quinazolines: a review, *Front. Chem.*, 2023, **11**, 1140562; (b) G. Sivakumar, A. K. Suresh and E. Balaraman, Tandem multicomponent reactions for diverse heterocycles synthesis under 3d-transition metal catalysis, in *Dehydrogenation Reactions with 3d Metals*, Springer Nature Switzerland, Cham, 2023, pp. 129–171; (c) N. Kumari, M. A. Hasan, B. D. Ward and L. Mishra, Reactivity of tetrabutylammonium iodide with a heteronuclear 6Cu(II)–4Na(I) complex: selective recognition of iodide ion, *Ind. Eng. Chem. Res.*, 2013, **52**, 15007–15014.
- 26 S. Dutt, V. Goel, N. Garg, D. Choudhury, D. Mallick and V. Tyagi, Biocatalytic Aza-Michael addition of aromatic amines to enone using α -amylase in water, *Adv. Synth. Catal.*, 2020, **362**, 858–866.
- 27 Q. Q. Wang, K. Xu, Y. Y. Jiang, Y. G. Liu, B. G. Sun and C. C. Zeng, Electrocatalytic Minisci acylation reaction of N-heteroarenes mediated by NH₄I, *Org. Lett.*, 2017, **19**, 5517–5520.
- 28 (a) S. Sharma, Vaishali, A. Pandey, S. Rani, P. Sharma, K. Mishra, A. Kumar, H. Kumar and A. Dhyani, An untold story of ionic liquid for the isatin derivative synthesis, *Curr. Org. Chem.*, 2025, **29**, 1240–1255; (b) G. Chen, H. J. Su, M. Zhang, F. Huo, J. Zhang, X. J. Hao and J. R. Zhao, New bactericide derived from isatin for treating oilfield reinjection water, *Chem. Cent. J.*, 2012, **6**, 90.
- 29 G. D. Allen, M. C. Buzzeo, C. Villagrán, C. Hardacre and R. G. Compton, A mechanistic study of the electro-oxidation of bromide in acetonitrile and the room-temperature ionic liquid 1-butyl-3-methylimidazolium bis(trifluoromethylsulfonyl)imide at platinum electrodes, *J. Electroanal. Chem.*, 2005, **575**, 311–320.
- 30 I. Damljanović, D. Stevanović, M. Vukićević and R. D. Vukićević, Electrochemical bromochlorination of peracetylated glycals, *Carbohydr. Res.*, 2011, **346**, 2683–2687.

